PNAS PNAS PNAS PNAS

Isoleucine 309 acts as a C_4 catalytic switch that increases ribulose-1,5-bisphosphate carboxylase/oxygenase (rubisco) carboxylation rate in *Flaveria*

Spencer M. Whitney[a,1], Robert E. Sharwood[a,2], Douglas Orr[a], Sarah J. White[a], Hernan Alonso[a], and Jeroni Galmés[b]

[a]Research School of Biology, Australian National University, Canberra ACT 2601, Australia; and [b]Grup de Recerca en Biologia de les Plantes en Condicions Mediterrànies Universitat de les Illes Balears, 07122 Mallorca, Spain

Edited by George H. Lorimer, University of Maryland, College Park, MD, and approved July 27, 2011 (received for review June 13, 2011)

Improving global yields of important agricultural crops is a complex challenge. Enhancing yield and resource use by engineering improvements to photosynthetic carbon assimilation is one potential solution. During the last 40 million years C_4 photosynthesis has evolved multiple times, enabling plants to evade the catalytic inadequacies of the CO_2-fixing enzyme, ribulose-1,5-bisphosphate carboxylase/oxygenase (rubisco). Compared with their C_3 ancestors, C_4 plants combine a faster rubisco with a biochemical CO_2-concentrating mechanism, enabling more efficient use of water and nitrogen and enhanced yield. Here we show the versatility of plastome manipulation in tobacco for identifying sequences in C_4-rubisco that can be transplanted into C_3-rubisco to improve carboxylation rate (V_C). Using transplastomic tobacco lines expressing native and mutated rubisco large subunits (L-subunits) from *Flaveria pringlei* (C_3), *Flaveria floridana* (C_3-C_4), and *Flaveria bidentis* (C_4), we reveal that Met-309-Ile substitutions in the L-subunit act as a catalytic switch between C_4 (^{309}Ile; faster V_C, lower CO_2 affinity) and C_3 (^{309}Met; slower V_C, higher CO_2 affinity) catalysis. Application of this transplastomic system permits further identification of other structural solutions selected by nature that can increase rubisco V_C in C_3 crops. Coengineering a catalytically faster C_3 rubisco and a CO_2-concentrating mechanism within C_3 crop species could enhance their efficiency in resource use and yield.

CO_2 assimilation | *rbcL* mutagenesis | gas exchange | chloroplast transformation

The future uncertainties of global climate change and estimates of unsustainable population growth have increased the urgency of improving crop yields (1). One possible solution is to "supercharge" photosynthesis by improving the C_3 cycle (2, 3). Although a simple idea, this is a complex challenge that involves several possible alternatives. Many of these alternatives focus on enhancing the performance of the CO_2-fixing enzyme ribulose-1,5-bisphosphate (RuBP) carboxylase/oxygenase (rubisco), which catalyses the first step in the synthesis of carbohydrates. Despite its pivotal role, rubisco is a slow catalyst, completing only one to four carboxylation reactions per catalytic site per second in plants (4, 5). Moreover CO_2 not only is fixed through a complex catalytic process but also must compete with O_2. The oxygenation of RuBP produces 2-phosphoglycolate, whose recycling by photorespiration requires energy and results in the futile loss of fixed carbon [~30% of fixed CO_2 in many C_3 plants (6)].

To compensate for rubisco's catalytic limitations, plants invest as much as 25% of their leaf nitrogen in rubisco (7). This value is much lower in C_4 plants, where a biochemical CO_2-concentrating mechanism (CCM) elevates CO_2 around rubisco. This optimized microenvironment allows rubisco to operate close to its maximal activity, reducing O_2 competition. This CCM has enabled C_4 plants to evolve rubiscos with substantially improved carboxylation rates (V_C) relative to their C_3 ancestors, albeit at the expense of reducing CO_2 affinity [i.e., a higher apparent K_m for CO_2 (K_C)] (8, 9). As a consequence, C_4 plants require less rubisco, thereby enhancing nitrogen use with improvements in V_C correlating with improved efficiency in nitrogen use (10). In addition, the high concentration of CO_2 around rubisco allows C_4 plants to operate at lower CO_2 pressures within their leaf air spaces, thereby reducing their stomatal conductance requirements and the associated H_2O loss by transpiration. Indicative of these growth advantages, C_4 photosynthesis has evolved independently several times from multiple C_3 lineages during the last 20–40 million years (11, 12).

Following nature's example, a number of CO_2 transgenic approaches have been designed to emulate CCM strategies in C_3 plastids and improve rubisco performance (2). These approaches include elevating the CO_2 concentration within chloroplasts using recombinant CO_2/HCO_3^- transporters from cyanobacteria or engineering alternative pathways to bypass photorespiration and release CO_2 within the stroma (13, 14). Although each strategy faces continuous challenges in its fine tuning and integration into crops, further improvements in yield and in the efficiency of water and nitrogen use are likely by concurrently "speeding up" rubisco (9).

Identifying the natural changes that result in the faster C_4 rubiscos is far from simple, given the complex structure and biogenesis pathway of the hexadecameric rubisco (L_8S_8) in vascular plants, whose assembly requirements cannot be met by conventional bacterial or in vitro expression systems (15). The catalytic core of L_8S_8 rubisco comprises four 52-kDa large (L)-subunit pairs which are capped by two sets of 15-kDa small (S)-subunit tetramers that provide structural stability and influence catalysis (16, 17). Although supplementing rice rubisco with S-subunits from the C_4 plant sorghum was found to improve V_C of the heterologous L_8S_8 enzyme (16), crosses between C_3 and C_4 *Flaveria* and *Atriplex* species showed C_4 catalysis to be maternally inherited (18, 19) and hence defined by the chloroplast-encoded L-subunit gene (*rbc*L). Therefore, changes in both Rubisco L- and S-subunits can influence catalysis.

Although phylogenetic studies have identified potential L-subunit residues involved in the transition from C_3-like to C_4-like rubisco, it is uncertain which residues are catalytically determinant (11, 20). Here we undertake a transplastomic approach to identify such residues in vivo. By manipulating the *rbc*L gene in tobacco to produce hybrid $L_8^FS_8^t$ rubiscos (containing variant *Flaveria* L- and tobacco S-subunits), we demonstrate that Met-309-Ile substitutions in the L-subunit act as

Author contributions: S.M.W. designed research; S.M.W., R.S., D.O., S.J.W., H.A., and J.G. performed research; S.M.W. and J.G. analyzed data; and S.M.W., R.S., H.A., and J.G. wrote the paper.

The authors declare no conflict of interest.

This article is a PNAS Direct Submission.

[1]To whom correspondence should be addressed. E-mail: Spencer.Whitney@anu.edu.au.

[2]Present address: Hawkesbury Institute for the Environment, University of Western Sydney, Richmond NSW 2753, Australia.

This article contains supporting information online at www.pnas.org/lookup/suppl/doi:10.1073/pnas.1109503108/-/DCSupplemental.

a catalytic switch between C_4 (^{309}Ile) and C_3 (^{309}Met) catalysis in *Flaveria* rubisco.

Results

***Flaveria* Rubisco L-Subunit Expression in Tobacco Chloroplasts.** The *rbc*L genes from *Flaveria pringlei* (C_3), *Flaveria floridana* (a C_3-C_4 intermediate), and *Flaveria bidentis* (C_4) were chosen for transformation into tobacco plastids because of their diverse catalytic properties (ref. 21 and below) despite their high sequence similarity (Fig. 1*A*). As in all *Flaveria rbc*L genes, nonsilent nucleotide changes occur only at residues 149, 265, and 309 (20). The *Flaveria* L-subunits show >95% identity with the tobacco L-subunit, with 22–24 amino acid differences in addition to a highly charged TDKDKDKKR extension at the C terminus (Fig S1). The *Flaveria rbc*L genes were cloned into the plastome-transforming plasmid pLEV4, where the expression of the transgenes is regulated by the native tobacco *rbc*L gene regulatory sequences [i.e., its promoter, 5′-, and 3′-untranslated sequences (22)]. The transforming plasmids, including the control pLEV4, were introduced biolistically into ^{cm}trL, a tailor-made tobacco master line for integrating *rbc*L transgenes into the tobacco chloroplast by homologous recombination (Fig. 1*B*) (23). Two independent transplastomic lines for each *rbc*L transgene were grown to maturity in soil in air supplemented with 0.5% (vol/vol) CO_2. The transformed tobacco lines that incorporated the *F. floridana*, *F. bidentis*, and *F. pringlei rbc*L genes were called "tob^{flo}," "tob^{bid}," and "tob^{pring}," respectively.

Nondenaturing PAGE (ndPAGE) analysis of the soluble leaf protein was used to confirm the production of the hybrid $L_8{}^FS_8{}^t$ rubisco (comprising *Flaveria* L-subunits and tobacco S-subunits) and to assesses the homoplasmicity of the tob^{pring}, tob^{flo}, and tob^{bid} lines (Fig. 1*C*). Each of the transformed lines examined was deemed to be homoplasmic, because no L_2 *Rhodospirillum rubrum* rubisco from the parental ^{cm}trL line was detected; homoplasmicity was further confirmed by DNA blot analysis (Fig S2).

Differential Expression of the Hybrid $L_8{}^FS_8{}^t$ Rubiscos. Differences in the intensities of the $L_8{}^FS_8{}^t$ bands in ndPAGE indicated that the amounts of rubisco produced in the T_0 lines varied (Fig. 1*C*). This variation was confirmed by quantitative [^{14}C]2-carboxyarabinitol-1,5-bisphosphate (CABP) binding. The amount of $L_8{}^FS_8{}^t$ produced in the tob^{flo}, tob^{bid}, and tob^{pring} leaves was reduced by approximately 50%, 65%, and 75% relative to wild-type, respectively (Fig. 1*C*). In contrast, rubisco content in the tob^{Lev4} control transformants matched that in wild-type, indicating that the additional genome changes around *rbc*L were not the cause of the reduced $L_8{}^FS_8{}^t$ expression. SDS PAGE-immunoblot analysis showed no unassembled *Flaveria* L-subunits accumulated as insoluble aggregates.

Contrary to the reduced $L_8{}^FS_8{}^t$ content in the T_0 leaves, there was little or no difference in the *Flaveria rbc*L mRNA levels in the same leaves relative to wild type (Fig. 1*D*), indicating that $L_8{}^FS_8{}^t$ synthesis probably is perturbed posttranscriptionally. As shown previously (23–25), a less abundant *rbc*L-*aad*A dicistronic mRNA (~10% that of the *rbc*L mRNA) was produced in all transformants as a result of inefficient transcription termination by the tobacco *rbc*L 3′UTR. The stages that hinder $L_8{}^FS_8{}^t$ expression during rubisco biogenesis or degradation remain to be identified fully.

Plant Growth and Leaf Photosynthesis. The disparity in $L_8{}^FS_8{}^t$ levels in leaves of the tob^{flo}, tob^{bid}, and tob^{pring} lines persisted to the T_2 progeny and correlated with their relative differences in photosynthesis and growth rates. For the tob^{flo} and tob^{bid} plants, the higher $L_8{}^FS_8{}^t$ levels produced were sufficient for them to survive through to maturity in air (without CO_2 enrichment), although they grew more slowly than wild-type plants (Fig. 2*A*). In contrast, the tob^{pring} transformants grew poorly in air. As seen

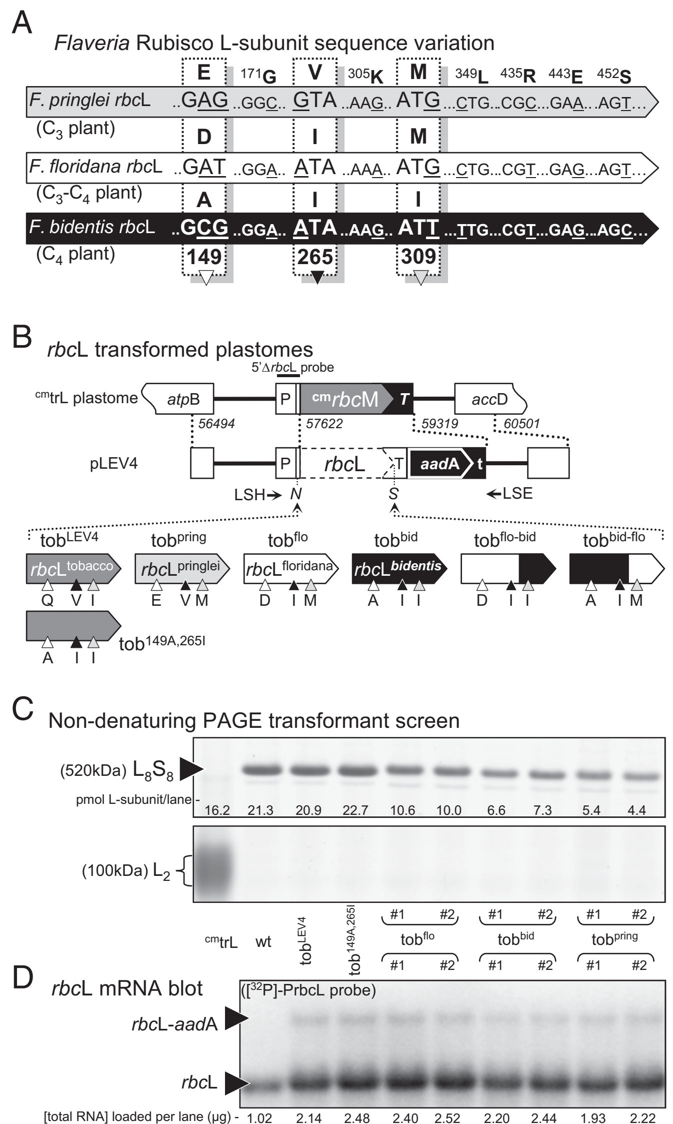

Fig. 1. *Flaveria* rubisco L-subunit sequence and expression in tobacco chloroplasts. (*A*) Comparison of Flaveria *rbc*L sequences that differ only in L-subunit substitutions at amino acids 149, 265, and 309 (20). (*B*) The transforming plasmid pLEV4 contains a homologous plastome flanking sequence (indicated by dashed lines; numbering indicates region of sequence integration relative to plastome sequence; GenBank ID Z00444) that directed integration of the *rbc*L transgenes and a promoterless *aad*A-selectable marker gene into the plastome of the tobacco master line, ^{cm}trL (23). The L-subunit amino acid differences at residues 149 (white triangle), 265 (black triangle), and 309 (gray triangle) in the tob^{LEV4} (tobacco *rbc*L control), tob^{pring} (*F. pringlei rbc*L), tob^{flo} (*F. floridana rbc*L), tob^{bid} (*F. bidentis rbc*L), tob$^{flo-bid}$ (chimeric *F. floridana*–*F. bidentis rbc*L), tob$^{bid-flo}$ (chimeric *F. bidentis*–*F. floridana rbc*L), and tob^{149A,265I} (mutated tobacco *rbc*L) transplastomic tobacco (tob) lines are shown. Annealing locations of primers LSH, LSE, and the 5′ Δ*rbc*L probe (24) are shown. N, NheI; S, SalI cloning sites. (*C*) Nondenaturing PAGE analysis of soluble protein from comparable leaves of independent T_0 transplastomic lines, ^{cm}trL, and wild-type tobacco (protein from 1.5 mm^2 of leaf was loaded per lane). Homoplasmic transformants produce only L_8S_8 rubisco (~520 kDa) and not the ~100-kDa *R. rubrum* L_2 rubisco produced in ^{cm}trL (23). (*D*) Detection of *rbc*L and *rbcL-aad*A mRNA in total RNA from 3 mm^2 (for wild type) or 6 mm^2 (other samples) of the leaves sampled in *C*.

previously in tobacco^{Rst} lines producing hybrid $L_8{}^sS_8{}^t$ rubisco (comprising sunflower L- and tobacco S-subunits) (24), the juvenile tob^{pring} plants displayed a pale green leaf phenotype with marginal curling and dimpling (Fig. 2*A Right*). This phenotype is

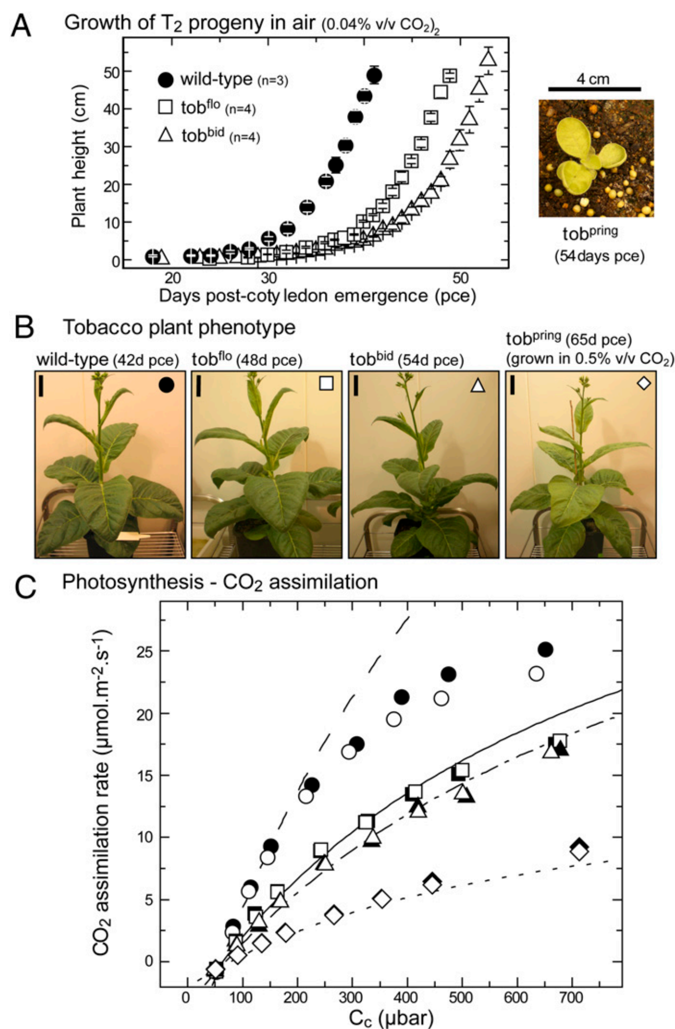

Fig. 2. Measurements of growth and leaf gas exchange in the transformants producing the variant $L^F{}_8S^t{}_8$ rubiscos. (*A*) (*Left*) Comparatively slower growth in air of the tob^{Flaveria} transformants as a function of plant height relative to wild-type. (*Right*) The tob^{pring} lines grew extremely poorly in air. pce, post-cotyledon emergence. (*B*) Phenotype of the plants from *A* at age pce as shown. (Scale bars: 4 cm.) Air supplemented with 0.5% (vol/vol) CO_2 was used to grow tob^{pring} plants to maturity. (*C*) Comparative differences in gas-exchange measurements of CO_2 assimilation rates at 25 °C under varying chloroplast CO_2 pressures (C_c) at growth illumination (400 μmol quanta $m^{-2} \cdot s^{-1}$). Measurements were made on young mature leaves located at similar canopy positions (fifth leaf from the apical meristem) of physiologically comparable mature plants analogous to those shown in *B*. Leaf rubisco contents were 25.0 and 30.5; 12.4 and 11.9; 10.1 and 10.8; 4.1 and 4.3 μmol rubisco sites m^{-2} in the independent wild-type (circles), tob^{flo} (squares; line 1 white, line 2 black), tob^{bid} (triangles; line 1 white, line 2 black), and tob^{pring} (diamonds; line 1 white, line 2 black) plants analyzed, respectively. The lines show the rubisco limited CO_2 assimilation rates for wild-type (– –), tob^{flo} (—),tob^{bid} (– · –), and tob^{pring} (....) modeled according to ref. 26 using the catalytic parameters for the respective hybrid $L^F{}_8S^t{}_8$ rubiscos in Fig. 3 and assuming rubisco was fully activated and a value of 0.3 mol $m^{-2} \cdot s^{-1} \cdot bar^{-1}$ for mesophyll conductance.

likely a consequence of the very low $L_8{}^FS_8{}^t$ content during early vegetative growth (<3 μmol sites $m^{-2} \cdot s^{-1}$) and in the young mature leaves (<6 μmol sites $m^{-2} \cdot s^{-1}$; Fig. 2*C*) of the tob^{pring} plants. Consistent with their different growth rates and varied $L_8{}^FS_8{}^t$ contents, the leaf photosynthetic CO_2 assimilation rates at varying CO_2 partial pressures (pCO_2) were slowest for tob^{pring} [but still slightly higher than in tobacco^{Rst} (24)] and were successively better for the tob^{bid} and tob^{flo} lines, albeit still slower than in wild-type tobacco (Fig. 2*C*). Measurements of the ratio of variable fluorescence to maximal fluorescence (F_v/F_m) in wild-type leaves (0.82 ± 0.01) were identical to those in the three tob^{Flaveria} genotypes (0.83 ± 0.01), indicating no difference in photochemical efficiency under the growth conditions.

Catalysis by Each $L_8{}^FS_8{}^t$ Rubisco Matches the Source *Flaveria* Enzyme. The catalytic properties of the recombinant $L_8{}^FS_8{}^t$ were compared with the source $L_8{}^FS_8{}^F$ enzymes from the corresponding *Flaveria* species (Fig. 3). As seen previously for the $L_8{}^sS_8{}^t$ rubisco produced in tobacco^{Rst} (24), the $L_8{}^FS_8{}^t$ and equivalent *Flaveria* $L_8{}^FS_8{}^F$ enzymes were catalytically comparable with respect to their carboxylation (V_C) and oxygenation (V_O) rates, their apparent Michaelis constants (K_m) for CO_2 (K_C) and O_2 (K_O), and CO_2/O_2 specificities ($S_{C/O}$). Of particular interest was the faster carboxylation rate (~35% higher V_C relative to the C_3 rubiscos) and lower CO_2 affinity (~50% higher K_C) of the hybrid $L_8{}^FS_8{}^t$ rubisco from tob^{bid} that matched the *F. bidentis* $L_8{}^FS_8{}^F$ enzyme (Fig. 3). As expected, when the catalytic properties and content of each $L_8{}^FS_8{}^t$ hybrid enzyme were used to model CO_2 assimilation rates according to Farquhar et al (26), the final values closely matched those measured by whole-leaf gas exchange (Fig. 2*C*). These results provide confidence both in the accuracy of the measured catalytic properties of the $L_8{}^FS_8{}^t$ hybrid enzymes and the rubisco-limited CO_2-assimilation model.

Interchanging C_3–C_4 Catalysis via ^{309}Met-^{309}Ile Substitutions in *Flaveria* Rubisco. The catalytic similarity between native *F. bidentis* rubisco and the hybrid tob^{bid} $L_8{}^FS_8{}^t$ enzyme indicated that the introduced L-subunit determined the catalytic phenotype. Because the *F. bidentis* and *F. floridana* L-subunits differ only at residues 149 and 309 but show significant differences in V_C and K_C (Fig. 3), domain swapping of their *rbc*L was used to identify which residue(s) imparted the C_4 catalysis of *F. bidentis* rubisco. The chimeric *rbc*L gene in the transforming plasmid pLEV$^{flo\text{-}bid}$ introduced a Met-309-Ile substitution into the *F. floridana rbc*L gene, whereas in pLEV$^{bid\text{-}flo}$ the chimeric *rbc*L gene coded an Ile-309-Met substitution in the *F. bidentis rbc*L gene (Fig. 1*B*). Both plasmids were transformed into ^{cm}trL, and

Plant line	Rubisco structure	L-subunit residue 149	265	309	K_C (μM)	V_C (s^{-1})	K_O (μM)	$^*S_{C/O}$ (mol.mol^{-1})	V_O (s^{-1})
N. tabacum (C_3)	$L^t{}_8S^t{}_8$	Q	V	I	12.6 ± 0.2	3.2 ± 0.2	274 ± 18	81 ± 1	0.8
tob^{149A,265I}	$L^t{}_8S^t{}_8$	A	I	I	12.2 ± 0.5	3.4 ± 0.2	306 ± 33	82 ± 1	1.1
F. pringlei (C_3)	$L^F{}_8S^F{}_8$	E	V	M	13.7 ± 0.5	3.5 ± 0.3	376 ± 35	81 ± 1	1.0
tob^{pring}	$L^F{}_8S^t{}_8$				13.0 ± 0.4	3.5 ± 0.3	317 ± 30	80 ± 2	1.1
F. floridana (C_3-C_4)	$L^F{}_8S^F{}_8$	D	I	M	14.4 ± 0.5	3.6 ± 0.1	374 ± 33	82 ± 2	1.1
tob^{flo}	$L^F{}_8S^t{}_8$				14.5 ± 0.3	3.7 ± 0.2	359 ± 22	81 ± 2	1.2
F. bidentis (C_4)	$L^F{}_8S^F{}_8$	A	I	I	20.4 ± 0.5	4.8 ± 0.3	420 ± 37	81 ± 1	1.2
tob^{bid}	$L^F{}_8S^t{}_8$				19.9 ± 0.6	4.7 ± 0.2	408 ± 28	79 ± 2	1.2
tob$^{flo\text{-}bid}$	$L^{cF}{}_8S^t{}_8$	D	I	I	19.3 ± 0.3	4.6 ± 0.2	393 ± 20	80 ± 1	1.2
tob$^{bid\text{-}flo}$	$L^{cF}{}_8S^t{}_8$	A	I	M	13.8 ± 0.3	3.7 ± 0.2	372 ± 24	81 ± 1	1.2

C_3-like catalysis (light bars): *N. tabacum*, tob^{149A,265I}, *F. pringlei*, tob^{pring}, *F. floridana*, tob^{flo}, tob$^{bid\text{-}flo}$. C_4-like catalysis (black bars): *F. bidentis*, tob^{bid}, tob$^{flo\text{-}bid}$.

Fig. 3. Comparative catalysis at 25 °C of the wild-type and $Q^{149}A$-$V^{265}I$ mutated tobacco ($L^t{}_8S^t{}_8$) rubisco, the source *Flaveria* ($L^F{}_8S^F{}_8$) rubiscos, the hybrid ($L^F{}_8S^t{}_8$, comprising *Flaveria* L- and tobacco S-subunits), and chimeric ($L^{cF}{}_8S^t{}_8$, comprising chimeric *Flaveria* L- and tobacco S-subunits) rubisco variants produced in the transplastomic tobacco plants. The L-subunit amino acid residues at codons 149, 265, and 309 in each rubisco type are shown. Values shown are the average ± SD of independent assays (*n* = 4–24; see *Materials and Methods* for details). The maximal oxygenation rate (V_O) was calculated using the equation $S_{C/O} = (V_C/K_C)/(V_O/K_O)$.

Fig. 4. Conservation and location of the L-subunit residues 149 and 309 in higher plant rubisco. (*A*) Coding matrix summary of ClustalW-aligned residues 300–319 in L-subunit sequences from data sets with corresponding C_3 and C_4 speciation data (11, 20, 38). (*B*) Structure of spinach L_8S_8 rubisco and L_8 core (L-subunits are shown in green; S-subunits are shown in blue) viewed from the top, showing central solvent channel (*Left* and *Center*), and from the side (*Right*). The relative locations of ^{149}Gln (white triangle) and ^{309}Met (yellow triangle) in one L-subunit pair (L_2) is shown. The ^{309}Met residues are located at the interface of L-subunits; the ^{149}Gln residues are positioned at the L_2–L_2 interface toward the surface of the central solvent channel. (*C*) View of an L-subunit pair (L_1 in green showing ribbon structural detail; L_2 in blue) showing the positioning of ^{149}Gln and ^{309}Met relative to each Mg^{2+} (black sphere) and the reaction-intermediate analog 2-CABP (yellow and red ball and stick) bound to the two active sites in the dimer. The conserved active-site residues are shown for one active site. Distances (in Å) from the S atom of ^{309}Met in L_2 to each Mg^{2+} and the Cα atom of the closest conserved active-site residue, ^{295}Arg, are shown. (This figure was prepared with PyMOL using the PDB co-ordinates 8RUC.)

independent tob$^{flo\text{-}bid}$- and tob$^{bid\text{-}flo}$-transformed tobacco lines were produced that grew to reproductive maturity in air.

Catalytic analysis of the chimeric ($L_8{}^{cF}S_8{}^{t}$) rubisco produced in the tob$^{flo\text{-}bid}$ T_1 progeny showed that the Met-309-Ile substitution increased V_C and K_C, matching that measured for the *F. bidentis* and tob^{bid} C_4-like rubiscos (Fig. 3). In contrast, introducing an Ile-309-Met mutation into the *F. bidentis* L-subunit (tob$^{bid\text{-}flo}$ lines) reduced V_C and K_C, resulting in a rubisco with C_3-like catalysis. These results demonstrate that ^{309}Ile confers *Flaveria* rubisco with C_4-like catalysis. Although a comparison of higher plant L-subunits shows that ^{309}Met is highly conserved in most C_3-plant rubiscos, the tobacco L-subunit encodes ^{309}Ile (Fig. 4*A*).

Amino Acid 149 Is Catalytically Neutral but Can Influence Rubisco Expression. The matching C_4-like catalysis of rubisco from tob$^{flo\text{-}bid}$ and tob^{bid} and C_3-like catalysis of the tob$^{bid\text{-}flo}$, tob^{flo}, and tob^{pring} rubiscos suggests that changes to amino acid 149 in *Flaveria* rubisco are catalytically neutral and possibly account for the amino acid heterogeneity at this position (Fig. 1*A*) (20). Likewise, conservation of ^{265}Ile in *F. floridana* and *F. bidentis* rubisco indicates that this residue also is catalytically neutral. The influence of Gln-149-Ala and Val-265-Ile L-subunit substitutions (to match those in *F. bidentis* rubisco; Fig. 1*B*) on tobacco rubisco were tested by transforming ^{cm}trL with the pLEV^{149A,265I}. Catalysis by rubisco in the tob^{149A,265I} lines matched that of the wild-type enzyme, demonstrating that both substitutions are catalytically neutral and are not able to impart C_4-like catalysis on tobacco rubisco (Fig. 3).

Despite the apparent neutrality of amino acid 149 on catalysis, changes at this position affected the level of the hybrid $L_8{}^{F}S_8{}^{t}$ expression. In young mature leaves of both tob$^{flo\text{-}bid}$ and tob^{flo}, whose L-subunits share ^{149}Asp (and ^{265}Ile), the rubisco levels were comparable (10–13 μmol sites $m^{-2}\cdot s^{-1}$). In contrast, the rubisco content in equivalent leaves from tob$^{bid\text{-}flo}$ and tob^{bid} (whose L-subunits code ^{149}Ala and ^{265}Ile) were lower (6–8 μmol sites $m^{-2}\cdot s^{-1}$) (Fig S3). These results suggest that changes to the amino acid (or its mRNA sequence) at residue 149 might be responsible for the variations in hybrid rubisco expression. However, this did not appear to be the case for tobacco Rubisco as the leaf Rubisco levels in the tob^{149A,265I} lines matched that in the wild-type leaves (Fig. 1*C*). How changes at residue 149 in the *Flaveria* L-subunit might differentially influence its translation, folding, and/or assembly with tobacco S-subunits or the stability of $L_8{}^{F}S_8{}^{t}$ complexes remains to be examined.

Discussion

Using transgenic tobacco lines expressing hybrid rubiscos containing *Flaveria* L- and tobacco S-subunits ($L_8{}^{F}S_8{}^{t}$), we have identified ^{309}Ile as the key residue that imparts C_4-like catalytic properties to *Flaveria* rubisco. The determinant role of this residue supports observations from prior crossing studies that showed C_4 catalysis to be maternally inherited in *Flaveria* (19). Linkages between catalysis and sequence phylogenies of different *Flaveria* rubisco L- and S-subunits indicated that C_4 catalysis was associated with two positively selected L-subunit amino acid substitutions: Asp-149-Ala and Met-309-Ile (20). Here we show that amino acid differences at position 149 in *Flaveria* rubisco probably are catalytically silent, because interchanging ^{149}Ala with ^{149}Asp in the L-subunit from either *F. floridana* or *F. bidentis* rubisco had no influence on catalysis (Fig. 3). Similarly, tobacco rubisco catalysis was unaffected by Q149A and V265I substitutions (Fig. 3).

A structural/functional explanation for how ^{309}Ile increases V_C in *Flaveria* rubisco is unclear. The similar positioning of conserved catalytic site residues in the crystal structures of catalytically different rubiscos makes it difficult to rationalize how distant changes influence catalysis (4, 20). The structure for spinach L_8S_8 rubisco (Fig. 4*B*) shows ^{309}Met located at the L-interface (i.e., between the L-subunits in each L_2 dimer) more than 17 Å away from the Mg^{2+} bound to each catalytic site and at least 13 Å away from the nearest conserved active site residue, ^{295}Arg (Fig. 4*C*). In contrast, ^{149}Gln is located further away from the active sites and close to the interface of the adjoining L_2 dimers that form the L_8 core (Fig. 4*B*). In the absence of a crystal structure for a *Flaveria* rubisco, it is difficult to explain how in-

PNAS PNAS PNAS

sertion of a more hydrophobic ^{309}Ile this far from the active site might influence V_C (20).

Despite the improvements in V_C imparted by ^{309}Ile in hybrid $L_8{}^F S_8{}^t$ rubisco, the accompanying reductions in CO_2 affinity (i.e., increased K_C) precluded gains in carboxylation efficiency. At 25 °C under ambient oxygen levels, the carboxylation efficiency (i.e., $V_C/K_C{}^{21\%O2}$) of the C_4-like ^{309}Ile-containing rubiscos in tob^{bid} and tob$^{flo\text{-}bid}$ (145 $mM^{-1}\cdot s^{-1}$) were poorer than the C_3-like ^{309}Met-$L_8{}^F S_8{}^t$ enzymes in tob^{pring} and tob^{flo} (150 and 161 $mM^{-1}\cdot s^{-1}$, respectively). Thus, because of the low CO_2 levels within (unstressed) C_3 chloroplasts (<10 μM), the faster C_4-like enzymes probably provide no advantage to plant growth within a C_3 plant (at least at 25 °C), as shown recently in rice (16). As modeled recently, optimal CO_2 concentrations required for C_4 rubisco are substantially higher (~80 μM) (8), indicating that taking full advantage of a faster rubisco in a C_3 plant will require the combinatorial effect of a suitable CCM, for which a number of strategies are being pursued (2). Some of these approaches already have demonstrated that elevating CO_2 pressures within C_3 plastids can improve the capacity for CO_2 assimilation by reducing the energy costs of photorespiration (13, 14).

Our results suggest that the carboxylation rate of rubisco in a C_3 plant might be increased either by direct replacement with L-subunits sourced from C_4 plants (as in the tob^{bid} plants; Fig. 3) or by tailoring appropriate sequence mutations into related C_3 rubisco L-subunits (as in the tob$^{flo\text{-}bid}$ plants; Fig. 3). Although the first approach suffers from our inability to predict a priori the assembly properties of foreign rubiscos within the chloroplast of the recipient transplastomic line, the second approach would require knowing the catalytic/structural effect of every possible mutation within the context of a particular rubisco enzyme, an understanding that we are still far from achieving. Indeed, the finding that tobacco rubisco encodes ^{309}Ile but shows C_3 catalysis highlights the complex natural variation in the sequence–structure–function relationships among plant L-subunits. Even the sequence diversity at position 309 among C_4 rubiscos (Fig. 4*A*) indicates that this residue is not the only one that can impart C_4 catalysis. This result is consistent with the polyphyletic evolution of C_4 photosynthesis (12) and with predictions that at least eight L-subunit residues (including residue 309 but not residue 149) have been selected for positively by C_4 catalysis (11). Experimentally testing these predictions, identifying other catalytically determinant L-subunit residues, and exploring which particular rubiscos are affected by these changes have been hampered by the preferential location of *rbc*L in the plastome (27) and the small range of species whose plastomes can be transformed stably (28). However, as shown in this and previous studies (24, 29, 30), these experimental limitations may be circumvented by expressing hybrid rubiscos in tobacco plastids. The generality of this system for examining sequence–performance relationships within otherwise inaccessible, catalytically diverse foreign L-subunits remains to be explored fully.

Although this study demonstrates the pervasive role of the L-subunit in shaping catalysis in plant rubisco, the important role of the S-subunits on catalysis cannot be overlooked. The apparent catalytic neutrality of the tobacco S-subunit when assembled with heterologous L-subunits (Fig. 3) (24, 29, 30) contrasts with the recent success in shaping rice rubisco toward C_4-like catalysis using heterologous S-subunits from C_4 sorghum (16). Similarly, structural changes to the S-subunit have improved *Chlamydomonas* rubisco catalysis (17). As highlighted recently (20), differences in rubisco S-subunit sequence also may account for the catalytic deviation of *Flaveria palmeri* rubisco, whose L-subunit sequence matches that of tob$^{flo\text{-}bid}$ (coding ^{309}Ile) but shows C_3 catalysis.

The similar $S_{C/O}$ values determined for rubisco from *F. bidentis*, *F. floridana*, and *F. pringlei* (Fig. 3) in this study contrast with the slightly varying values determined previously ($S_{C/O}$ = 76 ± 1, 84 ± 1, and 81 ± 1 respectively) (21). The reason for this variation is unknown but may lie in alterations in the catalytic competence as a result of different purification processes (ion exchange chromatography versus ammonium sulfate fractionation), the final enzyme purity, and the length of ultra-cold storage (24). By using fresh rubisco rapidly purified to >95% homogeneity by ion exchange chromatography, our measured $S_{C/O}$ values were highly reproducible between preparations from independent biological replicates.

Here we present an *rbc*L engineering approach involving hybrid rubisco production in tobacco plastids to unravel the sequence and catalytic diversity of related C_3 and C_4 rubiscos from *Flaveria*. Future applications of this experimental system are focused on identifying sequence changes that account for the natural diversity of rubisco performance and testing the feasibility of transplanting these catalytic improvements into the rubisco L-subunits of agriculturally relevant crops. In particular, when coengineered with biotechnological strategies to elevate CO_2 around rubisco in C_3 plants, a faster rubisco may translate into improved efficiency in water and nitrogen use and the enhanced yields currently enjoyed by C_4 plants.

Materials and Methods

RuBP and [^{14}C]2-CABP were synthesized as described (31, 32). Protein content was measured using a dye-binding assay (Pierce) and BSA as a protein-standard.

Tobacco Plastome Transformation and Growth. The transforming plasmid pLEV4 directs the insertion of an *rbc*L gene and a promoterless *aad*A gene (coding spectinomycin resistance) into the tobacco plastome in place of the L_2 *Rhodospirillum rubrum* rubisco-coding ^{cm}*rbc*M gene in the plastome of the tobacco master line ^{cm}trL (Fig. 1*B*) (23). The *rbc*L gene from *F. bidentis, F. pringlei*, and *F. floridana* was PCR amplified from leaf genomic DNA [isolated using the DNeasy Plant Mini Kit (Qiagen)] with the primers 5′ NheIrbcL (5′-A*GCTAGC*GTTGGATTCAAAGCTGGTGTT-3′ [the NheI site that spans the *rbc*L codons 9 (Ala) and 10 (Ser) is shown in italics] and 3′ SalIrbcL (5′-T*GTCGAC*TGTTT**TTA**TCTCTTCTTATCCTTATCCT-3′ [the reverse complement of the *rbc*L stop codon is shown in bold, and the SalI site is shown in italics]. The 1,439-bp NheI–SalI *rbc*L products were cloned into pLEV4 to give the transforming plasmids pLEV^{pring}, pLEV^{flo}, and pLEV^{bid}. The plasmids pLEV$^{flo\text{-}bid}$ and pLEV$^{bid\text{-}flo}$ were made by interchanging the 569-bp SphI–SalI fragments of the *F. bidentis* and *F. floridana rbc*L genes (Fig. 1*B*). Mutations coding substitutions Gln-149-Ala and Val-265-Ile in the tobacco *rbc*L gene in pLEV4 were introduced using the QuikChange Site-Directed Mutagenesis Kit (Stratagene) to produce plasmid pLEVtob^{149A,265I}. All plasmids were sequenced using BigDye terminator sequencing at the Biomolecular Resource Facility, Australian National University (Canberra, Australia).

Each of the pLEV-derived plasmids was introduced biolistically into three leaves of ^{cm}trL1 as described (23), and three to seven independent spectinomycin-resistant plants were obtained for each mutant. Two independent plastome-transformed lines for each introduced *rbc*L gene were grown to maturity in soil in a growth atmosphere supplemented with 0.5% (vol/vol) CO_2 as described (24). At each generation the plants were fertilized artificially with wild-type pollen.

PAGE and Nucleotide Blot Analyses. The preparation and analysis of soluble leaf protein by SDS/PAGE, nondenaturing PAGE, and immunoblot analysis was performed as described (33). Total leaf genomic DNA was isolated using the DNeasy Plant Mini Kit and used to PCR amplify and sequence the transformed plastome region using primers 5′- CTATGGAATTCGAACCTGAACTT-3′ (LSH) and 5′- GAGGTGTGATACTTGGCTTGATTC-3′ (LSE) (Fig. 1*B*) (24). DNA blot analysis of the genomic DNA was used to confirm homoplasmicity (Fig S1). Total RNA was extracted from 0.5 cm^2 of leaf in 0.8 mL TRIzol (Invitrogen). Six per cent or 12% of the RNA was separated on denaturing formaldehyde gels (34). The RNA was blotted onto Hybond-N nitrocellulose membrane (GE Healthcare) and probed with a ^{32}P-labeled 5′ Δ*rbc*L probe (Fig. 1*B*) as described (24).

Rubisco Content and Catalytic Assessments. Rates of rubisco $^{14}CO_2$ fixation using soluble leaf protein extract were measured in 7-mL septum-capped scintillation vials in reaction buffer [50 mM Hepes-NaOH (pH 7.8), 10 mM $MgCl_2$, 0.5 mM RuBP] containing varying concentrations of $NaH^{14}CO_3$ (0–67 μM)

and O_2 (0–25%) (vol/vol), accurately mixed with nitrogen using Wostoff gas-mixing pumps as described (24, 33). Assays (0.5 mL total volume) were started by the addition of activated leaf protein, and the Michaelis constants (K_m) for CO_2 (K_C) and O_2 (K_O) were determined from the fitted data. Replicate measurements (n = 4–8) were made using protein preparations from two to four different leaves of independently transformed lines. For each sample the maximal rate of carboxylation (V_C) was extrapolated from the Michealis–Menten fit and then normalized by dividing the rate by the number of rubisco-active sites quantified by [^{14}C]2-CABP binding (35, 36). Rubisco CO_2/O_2 specificity ($S_{C/O}$) was measured as described (37), using freshly extracted rubisco, quickly purified by ion exchange chromatography (24), from at least two separate plants for each independently transformed line.

Growth and Photosynthesis Analysis. Wild-type (*Nicotiana tabacum* L. Petit Havana) and transplastomic tobacco lines were grown in growth chambers at 25 °C and 400 ± 50 μmol photons $m^{-2} \cdot s^{-1}$ as described (24) in air or 0.5% (vol/vol) CO_2-enriched air. Plant height from the soil surface to the apical meristem was measured until the first floral apertures emerged. Leaf photosynthesis and dark respiration rates in plants of comparable physiological development (45–50 cm in height; 14 or 15 leaves) were made in the growth chamber using an LI-6400 gas-exchange system (Li-COR) (24). The maximum quantum efficiency of PSII in dark-adapted leaves [variable fluorescence (F_v)/maximum fluorescence (F_m)] was measured in the same leaves using an LI-6400–40 Leaf Chamber Fluorometer.

ACKNOWLEDGMENTS. This research was supported by Australian Research Council Discovery Grant FT0991407 (to S.M.W.) and by project AGL2009-07999 (Plan Nacional, Spain) (to J.G.).

1. Edgerton MD (2009) Increasing crop productivity to meet global needs for feed, food, and fuel. *Plant Physiol* 149:7–13.
2. Raines CA (2011) Increasing photosynthetic carbon assimilation in C_3 plants to improve crop yield: Current and future strategies. *Plant Physiol* 155:36–42.
3. von Caemmerer S, Evans JR (2010) Enhancing C_3 photosynthesis. *Plant Physiol* 154: 589–592.
4. Andersson I, Backlund A (2008) Structure and function of Rubisco. *Plant Physiol Biochem* 46:275–291.
5. Parry M, Madgwick P, Carvalho J, Andralojc P (2007) Prospects for increasing photosynthesis by overcoming the limitations of Rubisco. *J Agric Sci* 145:31–43.
6. Zhu X-G, Portis AR, Long SP (2004) Would transformation of C_3 crop plants with foreign Rubisco increase productivity? A computational analysis extrapolating from kinetic properties to canopy photosynthesis. *Plant Cell Environ* 27:155–165.
7. Evans JR (1989) Photosynthesis and nitrogen relationships in leaves of C_3 plants. *Oecologia* 78:9–19.
8. Savir Y, Noor E, Milo R, Tlusty T (2010) Cross-species analysis traces adaptation of Rubisco toward optimality in a low-dimensional landscape. *Proc Natl Acad Sci USA* 107:3475–3480.
9. Whitney SM, Houtz RL, Alonso H (2011) Advancing our understanding and capacity to engineer nature's CO_2-sequestering enzyme, Rubisco. *Plant Physiol* 155:27–35.
10. Ghannoum O, et al. (2005) Faster Rubisco is the key to superior nitrogen-use efficiency in NADP-malic enzyme relative to NAD-malic enzyme C_4 grasses. *Plant Physiol* 137:638–650.
11. Christin P-A, et al. (2008) Evolutionary switch and genetic convergence on *rbc*L following the evolution of C_4 photosynthesis. *Mol Biol Evol* 25:2361–2368.
12. Sage RF, Christin PA, Edwards EJ (2011) The C_4 plant lineages of planet Earth. *J Exp Bot* 62:3155–3169.
13. Kebeish R, et al. (2007) Chloroplastic photorespiratory bypass increases photosynthesis and biomass production in *Arabidopsis thaliana*. *Nat Biotechnol* 25:593–599.
14. Lieman-Hurwitz J, Rachmilevitch S, Mittler R, Marcus Y, Kaplan A (2003) Enhanced photosynthesis and growth of transgenic plants that express *ict*B, a gene involved in HCO_3- accumulation in cyanobacteria. *Plant Biotechnol J* 1:43–50.
15. Mueller-Cajar O, Whitney SM (2008) Directing the evolution of Rubisco and Rubisco activase: First impressions of a new tool for photosynthesis research. *Photosynth Res* 98:667–675.
16. Ishikawa C, Hatanaka T, Misoo S, Miyake C, Fukayama H (2011) Functional incorporation of sorghum small subunit increases the catalytic turnover rate of rubisco in transgenic rice. *Plant Physiol* 156:1603–1611.
17. Spreitzer RJ, Peddi SR, Satagopan S (2005) Phylogenetic engineering at an interface between large and small subunits imparts land-plant kinetic properties to algal Rubisco. *Proc Natl Acad Sci USA* 102:17225–17230.
18. Berry JA (1983) Genetic control of the kinetic parameters of RuP2 carboxylase: Studies of a C3 and a C4 species and their F hybrid. *Carnegie Institution of Washington Annual Report* 82:96–99.
19. Hudson GS, et al. (1990) Comparisons of *rbc*L genes for the large subunit of ribulose-bisphosphate carboxylase from closely related C_3 and C_4 plant species. *J Biol Chem* 265:808–814.
20. Kapralov MV, Kubien DS, Andersson I, Filatov DA (2011) Changes in Rubisco kinetics during the evolution of C_4 photosynthesis in *Flaveria* (Asteraceae) are associated with positive selection on genes encoding the enzyme. *Mol Biol Evol* 28:1491–1503.
21. Kubien DS, Whitney SM, Moore PV, Jesson LK (2008) The biochemistry of Rubisco in *Flaveria*. *J Exp Bot* 59:1767–1777.
22. Alonso H, Blayney MJ, Beck JL, Whitney SM (2009) Substrate-induced assembly of *Methanococcoides burtonii* D-ribulose-1,5-bisphosphate carboxylase/oxygenase dimers into decamers. *J Biol Chem* 284:33876–33882.
23. Whitney SM, Sharwood RE (2008) Construction of a tobacco master line to improve Rubisco engineering in chloroplasts. *J Exp Bot* 59:1909–1921.
24. Sharwood RE, von Caemmerer S, Maliga P, Whitney SM (2008) The catalytic properties of hybrid Rubisco comprising tobacco small and sunflower large subunits mirror the kinetically equivalent source Rubiscos and can support tobacco growth. *Plant Physiol* 146:83–96.
25. Whitney SM, Andrews TJ (2003) Photosynthesis and growth of tobacco with a substituted bacterial Rubisco mirror the properties of the introduced enzyme. *Plant Physiol* 133:287–294.
26. Farquhar G, vonCaemmerer S, Berry J (1980) A biochemical-model of photosynthetic CO_2 assimilation in leaves of C_3 species. *Planta* 149:78–90.
27. Kanevski I, Maliga P (1994) Relocation of the plastid *rbcL* gene to the nucleus yields functional ribulose-1,5-bisphosphate carboxylase in tobacco chloroplasts. *Proc Natl Acad Sci USA* 91:1969–1973.
28. Maliga P, Bock R (2011) Plastid biotechnology: Food, fuel, and medicine for the 21st century. *Plant Physiol* 155:1501–1510.
29. Sharwood R, Whitney S (2010) *The Chloroplast: Basics and Applications*, ed Ca R (Springer Science, Dordrecht, The Netherlands), pp 285–306.
30. Zhang XH, et al. (2011) Hybrid Rubisco of tomato large subunits and tobacco small subunits is functional in tobacco plants. *Plant Sci* 180:480–488.
31. Kane HJ, Wilkin JM, Portis AR, Andrews TJ (1998) Potent inhibition of ribulose-bisphosphate carboxylase by an oxidized impurity in ribulose-1,5-bisphosphate. *Plant Physiol* 117:1059–1069.
32. Pierce J, Tolbert NE, Barker R (1980) Interaction of ribulosebisphosphate carboxylase/oxygenase with transition-state analogues. *Biochemistry* 19:934–942.
33. Whitney SM, Sharwood RE (2007) Linked Rubisco subunits can assemble into functional oligomers without impeding catalytic performance. *J Biol Chem* 282: 3809–3818.
34. Sambrook J, Fritsch EF, Maniatis T (2000) *Molecular Cloning: A Laboratory Manual* (Cold Spring Harbor Laboratory, Cold Spring Harbor, NY).
35. Ruuska S, et al. (1998) The interplay between limiting processes in C_3 photosynthesis studied by rapid-response gas exchange using transgenic tobacco impaired in photosynthesis. *Aust J Plant Physiol* 25:859–870.
36. Whitney SM, Andrews TJ (2001) Plastome-encoded bacterial ribulose-1,5-bisphosphate carboxylase/oxygenase (RubisCO) supports photosynthesis and growth in tobacco. *Proc Natl Acad Sci USA* 98:14738–14743.
37. Kane HJ, et al. (1994) An improved method for measuring the CO_2/O_2 specificity of ribulosebisphosphate carboxylase-oxygenase. *Aust J Plant Physiol* 21:449–461.
38. Christin P-A, et al. (2011) Complex evolutionary transitions and the significance of C_3-C_4 intermediate forms of photosynthesis in *Molluginaceae*. *Evolution* 65:643–660.